Statistica Sinica Preprint No: SS-2025-0285	
Title	Bi-optimal Quantile-based Test Planning for Accelerated Degradation Test Based on a Wiener Process
Manuscript ID	SS-2025-0285
URL	http://www.stat.sinica.edu.tw/statistica/
DOI	10.5705/ss.202025.0285
Complete List of Authors	Ya-Shan Cheng and Chien-Yu Peng
Corresponding Authors	Chien-Yu Peng
E-mails	chienyu@stat.sinica.edu.tw
Notice: Accepted author version.	

Bi-optimal Quantile-based Test Planning for Accelerated Degradation Test Based on a Wiener Process

Ya-Shan Cheng[1] and Chien-Yu Peng[2*†]
[1]Graduate Institute of Statistics, National Central University
[2]Institute of Statistical Science, Academia Sinica

February 11, 2026

Abstract

Under limited resources, the widely used V_{t_q}-optimal test plan determines the sample size, termination time, and number of measurements by minimizing the approximate variances of the estimated q-quantile, t_q, for highly reliable products. This approach is economically efficient when the V_{t_q}-optimal test plan simultaneously satisfies another optimality criterion through an appropriate choice of q. Therefore, we theoretically study a bi-optimal quantile-based test plan based on a Wiener process, which achieves 100% efficiency for two optimality criteria. The necessary and sufficient conditions for its existence and uniqueness are derived, which can then be used to determine the optimal test configuration for accelerated degradation tests. Two numerical examples are presented to illustrate the practical applicability of the proposed bi-optimal quantile-based test plan.

Keywords: Cost-constrained optimization, D-optimal frequency, Inverse Gaussian distribution, Monotonicity, Signal-to-noise ratio

*Corresponding author email: chienyu@stat.sinica.edu.tw

Ya-Shan Cheng, ORCID ID: 0009-0003-0681-0864
Chien-Yu Peng, ORCID ID: 0000-0002-0400-5015

†The authors are grateful to the Editor, the Associate Editor, and anonymous referees for their insightful and constructive comments. This work of Ya-Shan Cheng and Chien-Yu Peng was supported in part by the National Science and Technology Council of Republic of China (Taiwan) under Grant Number NSTC-114-2118-M-008-003-MY2 and NSTC-112-2118-M-001-005-MY2, respectively.

1 Introduction

Rapid advances in technology have greatly improved product quality across industries, which has led manufacturers to place a growing emphasis on the development of high-reliability products to maintain competitiveness. Ensuring long-term product quality is crucial for customer satisfaction and plays an important role in building and sustaining a company's reputation. Thus, manufacturers are expected to provide reliable lifetime information for their products. When the quality characteristics of high-reliability products are closely linked to the failure mechanism and degrade over time, precise inferences about lifetime information can be made by analyzing collected degradation data. Degradation analysis has gained increasing attention across diverse fields such as biomedical engineering, aerospace, renewable energy systems, industrial applications, and public health research. Applications of degradation models can be found in D'Hondt et al. (2014), Wang and Wong (2015), Prasad et al. (2018), Prasad, Gopika, and Shridharan (2020), and Cheng, Chen, and Lee (2025).

Before conducting a degradation test (DT), the initial test plan involves fundamental *decision variables* such as the sample size, termination time, and number of measurements. For accelerated DTs (ADTs), most plans focus on the *test configuration*, which includes the stress levels, sample allocations, and number of measurements at each stress level under a pre-specified total number of stress levels (e.g., Lim and Yum, 2011; Hu, Lee, and Tang, 2015; Tseng and Lee, 2016). However, the total sample size, termination time, and number of measurements in the initial test plan are often assumed to be given without consideration of the experimental costs. Hence, these decision variables need to be determined under a total cost constraint. After this step, the test configuration for ADTs can then be selected using existing approaches. Extensive discussions of degradation planning and analysis can be found in Bagdonavičius and Nikulin (2001), Nelson (2004), Meeker, Escobar, and Pascual (2022), and the references cited therein.

Test plans are often optimized with respect to specific criteria. For instance, D-optimality involves maximizing the determinant of the Fisher information matrix (FIM) or precisely estimating the underlying model parameters $\boldsymbol{\theta}$ (i.e., minimizing the volume of a Wald confidence ellipsoid for $\boldsymbol{\theta}$). V_Ξ-optimality involves minimizing the approximate variance of the estimator of Ξ, where Ξ denotes a quantity of interest. The criterion V_Ξ corresponds to the well-known c-optimality criterion in optimal design theory, as discussed in standard references such as Pukelsheim (1993) and Atkinson, Donev, and Tobias (2007). For practical applications, see Boulanger and Escobar (1994), Tseng, Tsai, and Balakrishnan (2011), Tsai, Tseng, and Balakrishnan (2012), Lim (2015), and Peng and Cheng (2021). Other optimality criteria are reviewed in Wu and Hamada (2021). However, most studies on optimizing test plans employ a single optimality criterion. If a business owner already has an optimal test plan with respect to one criterion, they may be interested in knowing for which other criteria it is also optimal, as this helps assess the overall quality of the test plan. Thus, a test plan that simultaneously satisfies more than one optimality criterion would be economically attractive. In particular, a bi-optimal test plan can help manufacturers develop a robust maintenance and service strategy for their products.

We herein propose a bi-optimal test plan under a total cost constraint and based on the V_{t_q}-optimality criterion. A V_{t_q}-optimal test plan can generally be found for a given fixed q. This means that such a V_{t_q}-optimal test plan can be considered as a function of q, which in turn allows the value q to be chosen according to another optimality criterion. Thus, a key issue is to find a value of q such that the corresponding V_{t_q}-optimal test plan simultaneously satisfies a second optimality. It is therefore of interest to investigate the existence and uniqueness of such a test plan. If such a test plan exists, we refer to it as a bi-optimal quantile-based test plan.

A Wiener process is used to illustrate the conditions for the existence and uniqueness of a bi-optimal quantile-based test plan using D-optimality. The lifetime distribution of the first hitting time for a Wiener process follows an inverse Gaussian (IG) distribution (Chhikara and Folks, 1989), but there is no explicit expression for the q-quantile of the IG distribution. Instead, a normalizing logarithmic transformation proposed by Whitmore and Yalovsky (1978) provides an excellent approximation to the q-quantile of the IG distribution. This simple approximation facilitates the derivation of a closed form for the bi-optimal q^* (defined in Section 3), which in turn ensures the existence and uniqueness of the bi-optimal quantile-based test plan. The resulting conditions for existence and uniqueness reveal clear relationships between the model parameters and the experimental costs.

The assumptions on test configuration in Lee, Tseng, and Hong (2020) are adopted to extend our results to fit the use of ADTs. The grid-search procedure used by Lee et al. (2020) can be replaced with the proposed bi-optimal quantile-based test plan, thereby reducing computational effort in practical applications. The optimal test configuration for ADTs can then be determined using standard numerical search methods.

The remainder of this article is organized as follows. Section 2 introduces an accelerated degradation model based on a Wiener process and derives the corresponding D- and V_Ξ-optimal test plans under cost constraints. Section 3 presents the derivation of the bi-optimal quantile-based test plan. Section 4 provides an explicit expression and theoretical properties of the bi-optimal quantile-based test plan for the Wiener process. Section 5 describes the optimal test configuration for ADTs based on the bi-optimal quantile-based test plan. Section 6 presents numerical examples that illustrate the applicability of the results. Concluding remarks are given in Section 7.

2 Model Formulation and Cost-Constrained Optimal Test Plans

Assume that there are l combinations of explanatory (or accelerating) variables for ADTs. Let $\{Y(t;S_k); t \geq 0\}$ be a Wiener process in the kth experimental setting S_k $(k = 1, \ldots, l)$. The $Y(t;S_k)$ follows a normal distribution with mean $\eta(S_k)t$ and variance $\sigma^2(S_k)t$ (represented by $Y(t;S_k) \sim \mathcal{N}(\eta(S_k)t, \sigma^2(S_k)t))$, where $\eta(S_k)$ and $\sigma^2(S_k)$ denote the drift rate and dispersion functions, respectively, of S_k. Let $\boldsymbol{X}_k = (1, X_{k,1}, \ldots, X_{k,N_1-1})'$ and $\boldsymbol{Z}_k = (1, Z_{k,1}, \ldots, Z_{k,N_2-1})'$ respectively denote the (column) vectors of standardized explanatory variables in the kth experimental setting associated with the drift-rate and dispersion functions, where $X_{k,r}$ and $Z_{k,s}$ are functions of one or more standardized explanatory variables $(r = 1, \ldots, N_1 - 1,\ s = 1, \ldots, N_2 - 1)$ and the transpose symbol "$'$". Let $\boldsymbol{\beta} = (\beta_0, \beta_1, \ldots, \beta_{N_1-1})'$ and $\boldsymbol{\gamma} = (\gamma_0, \gamma_1, \ldots, \gamma_{N_2-1})'$ be the vectors of unknown parameters (or regression coefficients) and $\boldsymbol{\theta} = (\boldsymbol{\beta}', \boldsymbol{\gamma}')'$. Then, the following relationship can be assumed between the parameter functions and standardized explanatory variables:

$$\eta(S_k) = g_1(\boldsymbol{X}_k'\boldsymbol{\beta}) \quad \text{and} \quad \sigma^2(S_k) = g_2(\boldsymbol{Z}_k'\boldsymbol{\gamma}),$$

where g_1 and g_2 are link functions. In practice, the choice of link functions depends on the purposes. For example, Tseng et al. (2011) used simple exp-linear regression and constant functions for g_1 and g_2 in ADTs, respectively. Note that S_0 denotes the normal-use conditions, i.e., $X_{0,r} = Z_{0,s} = 0$ for $r = 1, \ldots, N_1 - 1$, $s = 1, \ldots, N_2 - 1$.

Let $Y_i(t_{i,j,k}; S_k)$ denote the observation of the ith degradation path at time $t_{i,j,k}$ in the kth experimental setting, S_k, for $i = 1, \ldots, n_k$, $j = 1, \ldots, m$, where n_k is the sample size (i.e., the number of test units) for setting S_k, and m is the number of measurements performed for each unit. The termination time of each degradation path at S_k is assumed to be the same (i.e., $t_{i,m,k} = t_{m,k}$). However, different degradation paths may have different measurement intervals before the termination time (i.e., $t_{i,1,k}, \ldots, t_{i,m-1,k}$). The total test units and total termination time are denoted by n and t_m, respectively, i.e., $\sum_{k=1}^{l} n_k = n$ and $\sum_{k=1}^{l} t_{m,k} = t_m$. The corresponding proportions of total test units and total termination time at S_k are denoted by $p_k = n_k/n \in [0, 1]$ and $\psi_k = t_{m,k}/t_m \in [0, 1]$, respectively. For simplicity, let $\boldsymbol{Y}_{ik} = (Y_i(t_{i,1,k}; S_k), \ldots, Y_i(t_{i,m,k}; S_k))'$ be the vector of observations of the ith degradation path corresponding to the kth setting. Hence, the single degradation path $\boldsymbol{Y}_{ik}$ follows an m-variate normal distribution:

$$\boldsymbol{Y}_{ik} \sim \mathcal{N}_m(g_1(\boldsymbol{X}_k'\boldsymbol{\beta})\boldsymbol{t}_{i,k}, g_2(\boldsymbol{Z}_k'\gamma)\boldsymbol{Q}_{i,k}), \tag{1}$$

where $\boldsymbol{t}_{i,k} = (t_{i,1,k}, \ldots, t_{i,m-1,k}, t_{m,k})'$ and $\boldsymbol{Q}_{i,k} = [\min\{t_{i,j_1,k}, t_{i,j_2,k}\}]_{1 \le j_1, j_2 \le m}$. The corresponding overall FIM, $\mathcal{I}_n(\boldsymbol{\theta})$, is expressed as a block diagonal matrix (see Supplementary Section 1.1),

$$\mathcal{I}_n(\boldsymbol{\theta}) = n((t_m\boldsymbol{B}) \oplus (m\boldsymbol{G}/2)), \tag{2}$$

where "$\oplus$" denotes the direct sum,

$$\boldsymbol{B} = \sum_{k=1}^{l} \frac{p_k\psi_k}{g_2(\boldsymbol{Z}_k'\gamma)} \left(\frac{\partial g_1(\boldsymbol{X}_k'\boldsymbol{\beta})}{\partial \boldsymbol{X}_k'\boldsymbol{\beta}}\right)^2 \boldsymbol{X}_k\boldsymbol{X}_k' \text{ and } \boldsymbol{G} = \sum_{k=1}^{l} \frac{p_k}{(g_2(\boldsymbol{Z}_k'\gamma))^2} \left(\frac{\partial g_2(\boldsymbol{Z}_k'\gamma)}{\partial \boldsymbol{Z}_k'\gamma}\right)^2 \boldsymbol{Z}_k\boldsymbol{Z}_k'.$$

Note that the block matrix $\boldsymbol{B}$ in the FIM does not depend on the intervening measurement times but relies on the termination time $t_{m,k}$ of each degradation path. Given $t_{m,k}$ and m for each S_k, the measurement intervals do not have to be equal for each sample. This flexibility allows for inspections to be conducted over arbitrary time periods in ADTs.

2.1 Cost-Constrained D-optimal Test Plan

The determinant of the FIM is expressed as

$$|\mathcal{I}_n(\boldsymbol{\theta})| = n^{N_1+N_2} \left|t_m \boldsymbol{B}\right| \left|\frac{m}{2}\boldsymbol{G}\right| = \frac{n^{N_1+N_2} t_m^{N_1} m^{N_2}}{2^{N_2}} \left|\boldsymbol{B}\right| \left|\boldsymbol{G}\right|, \tag{3}$$

where N_1 and N_2 represent the numbers of unknown parameters in the drift rate and dispersion functions, respectively. Their influence is reflected in the total termination time and number of measurements, respectively. Increasing the time span primarily improves the estimation of mean-value parameters, while increasing the number of observations improves the estimation of variance parameters by (2) and (3). The determinant depends on n through a power law due to the total number of parameters. Increasing n relative to t_m or m increases the amount of information obtained about the parameters involved in ADTs.

In real applications, the (accelerated) DT is constrained by the initial budget allocated to the experiment. A well-known total cost constraint proposed by Yu and Tseng (1999) is formulated as

$$\begin{aligned} &C_{op} t_m + C_{mea} mn + C_{it} n \leq C_b, \qquad (4) \\ &t_m \geq 0,\ m \geq 1,\ n \geq l, \end{aligned}$$

where the positive experimental costs C_{op}, C_{mea}, C_{it}, and C_b represent the cost of a time unit of operation, unit cost of each measurement, unit cost of a tested sample and the total budget, respectively. Without loss of generality, let $C_b = 1$. Note that the lower bound of n is the number of combinations of explanatory variables to fit the use of ADTs. When $l = 1$, it is the DT case. The upper bounds of the experimental costs C_{mea} and C_{it} are 1 (i.e., $0 < C_{mea}, C_{it} < 1$), but there is no upper bound for C_{op} as derived from (4). Applications using the total cost constraint can be found in Wu and Chang (2002), Liao and Tseng

(2006), Yang, Hsu, and Hu (2024), Cheng and Peng (2024), and Dong and Peng (2025).

Let $\boldsymbol{\xi} = (n, t_m, m)$ denote a test plan for $n \geq l$, $t_m \geq 0$, and $m \geq 1$. Because the determinant in (3) is factored into a product of model parameters and decision variables, this implies that the objective function is only proportional to the decision variables. Hence, the determinant in (3) can be generalized to the following objective function without loss of generality:

$$\mathbb{D}(\boldsymbol{\xi}) = n^{N_0} t_m^{N_1} m^{N_2},\ N_0, N_1, N_2 \in \mathbb{N}, \tag{5}$$

where the exponents N_0, N_1, and N_2 are given constants. When $l = 1$ for a DT without explanatory variables (i.e., $X_{k,r} = Z_{k,s} = 0$ for $r = 1, \ldots, N_1 - 1$, $s = 1, \ldots, N_2 - 1$), then $(N_0, N_1, N_2) = (2, 1, 1)$ (e.g., Peng and Cheng, 2021). Tseng et al. (2011) used $g_1(x) = \exp(\beta_0 + \beta_1 x)$ and $g_2(z) = \gamma_0$ for ADTs with a single accelerating variable x, which corresponds to $(N_0, N_1, N_2) = (3, 2, 1)$. According to (5), $\mathbb{D}(\boldsymbol{\xi})$ strictly increases with n, t_m, and m. Thus, some constraints are necessary for maximization problems.

Let X and $\boldsymbol{\xi}_X = (n_X, t_{m;X}, m_X)$ denote any (alphabetical) optimality criterion and the X-optimal test plan, respectively, under the total cost constraint in (4). Hence, the D-optimal test plan $\boldsymbol{\xi}_D$ maximizes $\mathbb{D}(\boldsymbol{\xi})$ in (5) subject to the total cost constraint in (4). According to (3) or (5), the model parameters do not influence the D-optimal test plan, which is robust to parameter uncertainty. All derivations of this article can be found in the supplementary file.

Theorem 2.1. *Given N_0, N_1, N_2, C_{op}, C_{mea}, and C_{it}, the D-optimal test plan $\boldsymbol{\xi}_D$ can be divided into two parts as follows:*

(i) For $N_0 > N_2$,

(1) $C_{it} + \frac{(N_1+N_2)C_{mea}}{N_2} < \frac{1}{l} \leq \frac{(N_0+N_1)C_{it}}{N_0-N_2}$ *if and only if*

$$\boldsymbol{\xi}_D = \left(l, \frac{N_1(1-lC_{it})}{(N_1+N_2)C_{op}}, \frac{N_2(1-lC_{it})}{(N_1+N_2)lC_{mea}}\right).$$

(2) $C_{mea} < \frac{N_2 C_{it}}{N_0-N_2}$ *and* $C_{it} < \frac{N_0-N_2}{l(N_0+N_1)}$ *if and only if*

$$\boldsymbol{\xi}_D = \left(\frac{N_0-N_2}{(N_0+N_1)C_{it}}, \frac{N_1}{(N_0+N_1)C_{op}}, \frac{N_2 C_{it}}{(N_0-N_2)C_{mea}}\right).$$

(3) $C_{mea} \geq \frac{N_2 C_{it}}{N_0-N_2}$ *and* $C_{it} + C_{mea} < \frac{N_0}{l(N_0+N_1)}$ *if and only if*

$$\boldsymbol{\xi}_D = \left(\frac{N_0}{(N_0+N_1)(C_{it}+C_{mea})}, \frac{N_1}{(N_0+N_1)C_{op}}, 1\right).$$

(4) $\frac{N_0}{l(N_0+N_1)} \leq C_{it} + C_{mea} < \frac{1}{l} \leq C_{it} + \frac{(N_1+N_2)C_{mea}}{N_2}$ *if and only if*

$$\boldsymbol{\xi}_D = \left(l, \frac{1-lC_{mea}-lC_{it}}{C_{op}}, 1\right).$$

(ii) *For* $N_0 \leq N_2$*,*

(1) $C_{it} + \frac{(N_1+N_2)C_{mea}}{N_2} < \frac{1}{l}$ *if and only if*

$$\boldsymbol{\xi}_D = \left(l, \frac{N_1(1-lC_{it})}{(N_1+N_2)C_{op}}, \frac{N_2(1-lC_{it})}{(N_1+N_2)lC_{mea}}\right).$$

(2) $C_{it} + C_{mea} < \frac{1}{l} \leq C_{it} + \frac{(N_1+N_2)C_{mea}}{N_2}$ *if and only if*

$$\boldsymbol{\xi}_D = \left(l, \frac{1-lC_{mea}-lC_{it}}{C_{op}}, 1\right).$$

Note that the feasible region for the D-optimal test plan is bounded by $C_{it} > 0$, $C_{mea} > 0$, and $C_{it} + C_{mea} < 1/l$ and shrinks with increasing l. Table 1 presents the monotonicity property of the D-optimal decision variables in Theorem 2.1(i) with respect to the constants N_0, N_1, and N_2 as well as experimental costs. Note that the monotonicity property of the

		N_0	N_1	N_2	C_{it}	C_{op}	C_{mea}			N_0	N_1	N_2	C_{it}	C_{op}	C_{mea}
(1)	$t_{m;D}$	0	+	−	−	−	0	(2)	n_D	+	−	−	−	0	0
	m_D	0	−	+	−	0	−		$t_{m;D}$	−	+	0	0	−	0
									m_D	−	0	+	+	0	−
(3)	n_D	+	−	0	−	0	−	(4)	$t_{m;D}$	0	0	0	−	−	−
	$t_{m;D}$	−	+	0	0	−	0								

Table 1: Monotonicity properties in the parameters and experimental costs for the D-optimal test plan in Theorem 2.1(i).

D-optimal decision variables in Theorem 2.1(ii) is the same as described by Theorem 2.1(i)-(1) and (4) and is therefore not included in Table 1. For Theorem 2.1(i)-(2), n_D is strictly increasing with N_0 and strictly decreasing with N_1, N_2, and C_{it}. $t_{m;D}$ is strictly decreasing with N_0 and C_{op} and increasing with N_1. m_D is strictly decreasing with N_0 and C_{mea} and increasing with N_2 and C_{it}. Similar explanations apply to the other cases (i.e., Theorem 2.1(i)-(1), (3) and (4)) presented in Table 1.

The necessary and sufficient conditions outlined in Theorem 2.1 do not depend on the experimental cost C_{op}. Thus, let the experimental costs C_{it} and C_{mea} be represented by the x-axis and y-axis, respectively. Figure 1 depicts the feasible regions of optimal test plans with the dividing functions representing the necessary and sufficient conditions described in Theorem 2.1. Different colored areas correspond to the different feasible regions for the D-optimal test plans as described in Theorem 2.1: khaki corresponds to the interior case $n_D > l$ and $m_D > 1$, pale-green corresponds to the boundary case $n_D = l$, pink corresponds to the boundary case $m_D = 1$; and the light-blue corresponds to the trivial case $n_D = l$ and

$m_D = 1$. In Figure 1(a), the intersection point P $= ((N_0 - N_2)/(l(N_0 + N_1)), N_2/(l(N_0 + N_1)))$ can be calculated by using the dividing functions $C_{mea} = N_2C_{it}/(N_0 - N_2)$ and $C_{it} = (N_0 - N_2)/(l(N_0 + N_1))$. As $N_0 - N_2 \to 0$ in Theorem 2.1(i), the intersection point P moves toward $(0, N_0/(l(N_0 + N_1)))$ in Figure 1(a), which simplifies to Figure 1(b). The corresponding result is reduced to Theorem 2.1(ii) (i.e., $n_D = l$).

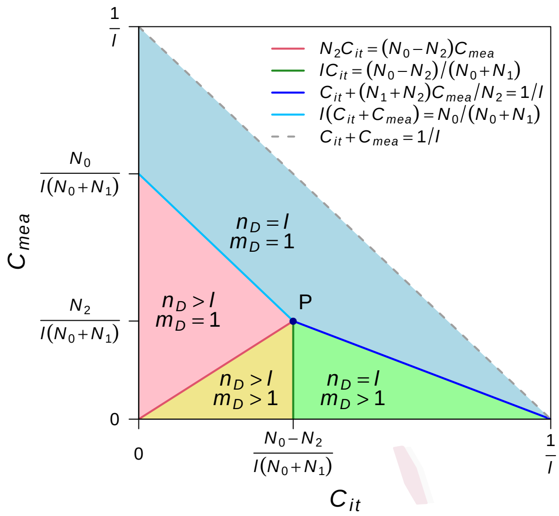

(a) $N_0 > N_2$

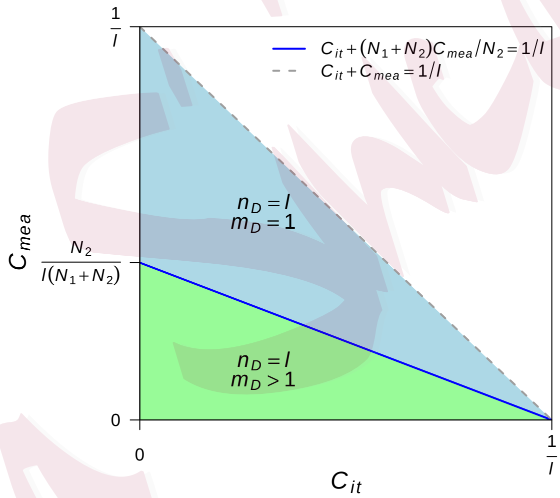

(b) $N_0 \leq N_2$

Figure 1: Feasible regions of D-optimal test plans

In practice, cost coefficients may vary. Thus, it is of interest to assess how often the alternatives (i.e., interior, boundary, and trivial cases) occur. To this end, we assume that the cost coefficients are uniformly distributed over a feasible region. Then, the feasible regions of the D-optimal test plans in Theorem 2.1 can be compared as follows. Based on the conditions in Theorem 2.1(i), let Ω be the sample space of the D-optimal test plan (i.e., the feasible region is enclosed by $C_{it} = 0, C_{mea} = 0$, and $C_{it} + C_{mea} = 1/l$). Let A_j be the area of the D-optimal test plan ξ_D in Theorem 2.1(i)-(j) for $j = 1, 2, 3, 4$. Therefore, we have $\Omega = \bigcup_{j=1}^{4} A_j$. The occurrence probabilities in Theorem 2.1(i) are easy to calculate as

$$\Pr(A_1) = \frac{N_2(N_1+N_2)}{(N_0+N_1)^2}, \quad \Pr(A_2) = \frac{N_2(N_0-N_2)}{(N_0+N_1)^2},$$
$$\Pr(A_3) = \frac{N_0(N_0-N_2)}{(N_0+N_1)^2}, \quad \Pr(A_4) = \frac{N_1(2N_0+N_1-N_2)}{(N_0+N_1)^2}.$$

A similar definition can be made for Theorem 2.1(ii).

Corollary 2.1. *Given the D-optimal test plan in Theorem 2.1.*

(i) For $N_0 > N_2$, the ratio of the cases in Theorem 2.1(i)-(1)–(4) is

$$\Pr(A_1) : \Pr(A_2) : \Pr(A_3) : \Pr(A_4) = \frac{N_1+N_2}{N_0-N_2} : 1 : \frac{N_0}{N_2} : \frac{N_1(2N_0+N_1-N_2)}{N_2(N_0-N_2)}.$$

Moreover, we have $\Pr(A_2) < \Pr(A_3)$.

(ii) For $N_0 \le N_2$, the ratio of the areas in Theorem 2.1(ii)-(1) and (2) is $N_2 : N_1$.

Corollary 2.1 provides a clear comparison of the occurrence probabilities of the different types of D-optimal test plans. It demonstrates that the interior case of the D-optimal test plan is not the most probable scenario.

For certain relationships among the exponents N_0, N_1, and N_2, the D-optimal test plan to the cost-constrained maximization problem leads to (partially) equal allocations of experimental cost.

Corollary 2.2. *Given the D-optimal test plan in Theorem 2.1.*

(i) For Theorem 2.1(i)-(1) and (ii)-(1), we have $N_2 C_{op} t_{m;D} = l N_1 C_{mea} m_D$.

(ii) For Theorem 2.1(i)-(2), (a) if $N_0 = N_1 + N_2$, then $C_{op} t_{m;D} = C_{it} n_D$; (b) if $N_0 = N_1 + N_2$ and $N_1 = N_2$ (i.e., $N_0 : N_1 : N_2 = 2 : 1 : 1$), then $C_{op} t_{m;D} = C_{mea} m_D n_D = C_{it} n_D = 1/3$.

(iii) For Theorem 2.1(i)-(3), we have $N_0 C_{op} t_{m;D} = N_1(C_{it} + C_{mea}) n_D$.

Corollary 2.2(ii)-(a) indicates that, under partially equal experimental cost allocations (i.e., $C_{op} t_{m;D} = C_{it} n_D$), an increase in the experimental cost C_{op} leads to a decrease in the D-optimal total termination time $t_{m;D}$, while an increase in the experimental cost C_{it} leads to a decrease in the D-optimal total sample size n_D. According to Corollary 2.2(ii)-(b), each experimental cost allocation occupies one third of the total budget.

2.2 Cost-Constrained V_Ξ-optimal Test Plan

Let $\Xi(\boldsymbol{\theta})$ be a real-valued and continuously differentiable function, and let $\nabla\Xi(\boldsymbol{\theta})$ be a non-zero vector with the gradient of Ξ evaluated at $\boldsymbol{\theta}$. Then, the invariance property of the maximum likelihood (ML) estimator (denoted by $\hat{\boldsymbol{\theta}}$), the delta method, and (2) can be used to the approximate the variance of $\Xi(\hat{\boldsymbol{\theta}})$:

$$\begin{aligned}
\mathrm{AVar}(\Xi(\hat{\boldsymbol{\theta}})) &= \nabla\Xi(\boldsymbol{\theta})'\mathcal{I}_n^{-1}(\boldsymbol{\theta})\nabla\Xi(\boldsymbol{\theta}) \\
&= \frac{1}{n}\begin{pmatrix} \frac{\partial\Xi(\boldsymbol{\theta})}{\partial\boldsymbol{\beta}'} & \frac{\partial\Xi(\boldsymbol{\theta})}{\partial\boldsymbol{\gamma}'} \end{pmatrix} \begin{bmatrix} \frac{\boldsymbol{B}^{\#}}{t_m|\boldsymbol{B}|} & \mathbf{0}_{N_1\times N_2} \\ \mathbf{0}_{N_2\times N_1} & \frac{2\boldsymbol{G}^{\#}}{m|\boldsymbol{G}|} \end{bmatrix} \begin{pmatrix} \frac{\partial\Xi(\boldsymbol{\theta})}{\partial\boldsymbol{\beta}} \\ \frac{\partial\Xi(\boldsymbol{\theta})}{\partial\boldsymbol{\gamma}} \end{pmatrix} \\
&= \frac{1}{n}\left(\frac{1}{t_m|\boldsymbol{B}|}\frac{\partial\Xi(\boldsymbol{\theta})}{\partial\boldsymbol{\beta}'}\boldsymbol{B}^{\#}\frac{\partial\Xi(\boldsymbol{\theta})}{\partial\boldsymbol{\beta}} + \frac{2}{m|\boldsymbol{G}|}\frac{\partial\Xi(\boldsymbol{\theta})}{\partial\boldsymbol{\gamma}'}\boldsymbol{G}^{\#}\frac{\partial\Xi(\boldsymbol{\theta})}{\partial\boldsymbol{\gamma}}\right) \\
&\propto \frac{1}{n}\left(\frac{1}{t_m} + \frac{\alpha_\Xi(\boldsymbol{\theta})}{m}\right),
\end{aligned} \tag{6}$$

where $\boldsymbol{B}^{\#}$ and $\boldsymbol{G}^{\#}$ denote the adjoint matrices of $\boldsymbol{B}$ and $\boldsymbol{G}$, respectively, and

$$\alpha_\Xi(\boldsymbol{\theta}) = \frac{2|\boldsymbol{B}|\frac{\partial\Xi(\boldsymbol{\theta})}{\partial\boldsymbol{\gamma}'}\boldsymbol{G}^{\#}\frac{\partial\Xi(\boldsymbol{\theta})}{\partial\boldsymbol{\gamma}}}{|\boldsymbol{G}|\frac{\partial\Xi(\boldsymbol{\theta})}{\partial\boldsymbol{\beta}'}\boldsymbol{B}^{\#}\frac{\partial\Xi(\boldsymbol{\theta})}{\partial\boldsymbol{\beta}}}. \tag{7}$$

The functional form presented in (6) highlights some important features relevant to the Wiener process. Information regarding the approximate variance of $\Xi(\hat{\boldsymbol{\theta}})$ can be summarized in a single function $\alpha_\Xi(\boldsymbol{\theta})$, which leads to a substantial simplification of $\text{AVar}(\Xi(\hat{\boldsymbol{\theta}}))$. The function $\alpha_\Xi(\boldsymbol{\theta})$ is called the integrated variance (IV) function (Dong and Peng, 2025).

Under normal-use conditions S_0 (i.e., $X_{0,r} = Z_{0,s} = 0$ for $r = 1, \ldots, N_1 - 1$, $s = 1, \ldots, N_2 - 1$), we have $\nabla\Xi(\boldsymbol{\theta}) = (\partial\Xi(\boldsymbol{\theta})/\partial\beta_0, \mathbf{0}'_{N_1-1}, \partial\Xi(\boldsymbol{\theta})/\partial\gamma_0, \mathbf{0}'_{N_2-1})'$, where $\mathbf{0}_{N_1-1}$ is a zero vector of length $N_1 - 1$. Then the IV function $\alpha_\Xi(\boldsymbol{\theta})$ in (7) is simplified to

$$\alpha_\Xi(\boldsymbol{\theta}) = \frac{2g^{(1,1)}\,|\boldsymbol{B}|\,(\partial\Xi(\boldsymbol{\theta})/\partial\gamma_0)^2}{b^{(1,1)}\,|\boldsymbol{G}|\,(\partial\Xi(\boldsymbol{\theta})/\partial\beta_0)^2}. \tag{8}$$

where $b^{(1,1)}$ represents the determinant of the $(N_1 - 1) \times (N_1 - 1)$ matrix obtained after removing the first row and first column from $\boldsymbol{B}$ and the same definition for $g^{(1,1)}$.

Without loss of generality, the V_Ξ-objective function is formulated as follows:

$$\mathbb{V}_\Xi(\boldsymbol{\xi}) = \frac{1}{n}\left(\frac{1}{t_m} + \frac{\alpha_\Xi(\boldsymbol{\theta})}{m}\right),\ \alpha_\Xi(\boldsymbol{\theta}) > 0. \tag{9}$$

Applications of the same functional form in (9) can be found in Peng and Cheng (2021) for the IG process in a DT, Lim and Yum (2011) for the Wiener process in ADTs, and Tseng and Lee (2016) for the Tweedie process in ADTs. To avoid parameter uncertainty in the V_Ξ-optimal test plan, the locally optimal design proposed by Chernoff (1953) is adopted, where the ML estimates are used to replace the unknown parameters in $\alpha_\Xi(\boldsymbol{\theta})$. The cost-constrained V_Ξ-optimization problem is to minimize $\mathbb{V}_\Xi(\boldsymbol{\xi})$ in (9) subject to the total cost constraint in (4). Following a similar proof of Theorem 2.1 proposed by Dong and Peng (2025), the V_Ξ-optimal test plan $\boldsymbol{\xi}_{V_\Xi}$ can be derived as follows.

Theorem 2.2. *Given $\alpha_\Xi(\boldsymbol{\theta})$, C_{op}, C_{mea}, and C_{it}, the V_Ξ-optimal test plan with the total cost constraint can be divided into four parts as follows:*

(i) The V_Ξ-optimal test plan is

$$\boldsymbol{\xi}_{V_\Xi} = \left(l, \frac{1 - lC_{it}}{C_{op} + \sqrt{\alpha_\Xi(\boldsymbol{\theta})C_{op}C_{mea}l}}, \frac{1 - lC_{it}}{lC_{mea} + \sqrt{lC_{op}C_{mea}/\alpha_\Xi(\boldsymbol{\theta})}}\right)$$

if and only if (a) $2C_{it} + C_{mea} < \dfrac{1}{l}$ *and* $\dfrac{(1-2lC_{it})^2 C_{op}}{l^3 C_{mea} C_{it}^2} \le \alpha_\Xi(\boldsymbol{\theta})$ *or*

(b) $C_{it} + C_{mea} < \dfrac{1}{l} \le 2C_{it} + C_{mea}$ *and* $\alpha_\Xi(\boldsymbol{\theta}) > \dfrac{lC_{mea}C_{op}}{(1 - lC_{it} - lC_{mea})^2}$.

(ii) The V_Ξ*-optimal test plan is* $\boldsymbol{\xi}_{V_\Xi} = (n(m_{\boldsymbol{\theta}}), t(m_{\boldsymbol{\theta}}), m_{\boldsymbol{\theta}})$*, where*

$$t(m_{\boldsymbol{\theta}}) = \frac{\sqrt{C_{op}m_{\boldsymbol{\theta}}(C_{op}m_{\boldsymbol{\theta}} + \alpha_\Xi(\boldsymbol{\theta}))} - C_{op}m_{\boldsymbol{\theta}}}{C_{op}\alpha_\Xi(\boldsymbol{\theta})},$$

$$n(m_{\boldsymbol{\theta}}) = \frac{C_{op}m_{\boldsymbol{\theta}} + \alpha_\Xi(\boldsymbol{\theta}) - \sqrt{C_{op}m_{\boldsymbol{\theta}}(C_{op}m_{\boldsymbol{\theta}} + \alpha_\Xi(\boldsymbol{\theta}))}}{\alpha_\Xi(\boldsymbol{\theta})(C_{mea}m_{\boldsymbol{\theta}} + C_{it})},$$

$$m_{\boldsymbol{\theta}} = \frac{C_{it}}{3C_{mea}} \left\{ \sqrt[3]{k_1(\alpha_\Xi(\boldsymbol{\theta})) + k_2(\alpha_\Xi(\boldsymbol{\theta}))} + \sqrt[3]{k_1(\alpha_\Xi(\boldsymbol{\theta})) - k_2(\alpha_\Xi(\boldsymbol{\theta}))} - 2 \right\},$$

with

$$k_1(\alpha_\Xi(\boldsymbol{\theta})) = \frac{27C_{mea}\alpha_\Xi(\boldsymbol{\theta})}{2C_{it}C_{op}} - 8,$$

$$k_2(\alpha_\Xi(\boldsymbol{\theta})) = \frac{3}{2}\sqrt{\frac{3C_{mea}\alpha_\Xi(\boldsymbol{\theta})}{C_{it}C_{op}}\left(\frac{27C_{mea}\alpha_\Xi(\boldsymbol{\theta})}{C_{it}C_{op}} - 32\right)}$$

if and only if $2C_{it} + C_{mea} < \dfrac{1}{l}$ *and* $\dfrac{(2C_{it} + C_{mea})C_{mea}C_{op}}{C_{it}^2} < \alpha_\Xi(\boldsymbol{\theta}) < \dfrac{(1-2lC_{it})^2 C_{op}}{l^3 C_{it}^2 C_{mea}}$.

(iii) The V_Ξ*-optimal test plan is*

$$\boldsymbol{\xi}_{V_\Xi} = \left(\frac{C_{op} + \alpha_\Xi(\boldsymbol{\theta}) - \sqrt{C_{op}(C_{op} + \alpha_\Xi(\boldsymbol{\theta}))}}{\alpha_\Xi(\boldsymbol{\theta})(C_{it} + C_{mea})}, \frac{\sqrt{C_{op}(C_{op} + \alpha_\Xi(\boldsymbol{\theta}))} - C_{op}}{\alpha_\Xi(\boldsymbol{\theta})C_{op}}, 1 \right)$$

if and only if $2C_{it} + C_{mea} < \dfrac{1}{l}$ *and* $\dfrac{(2l(C_{it} + C_{mea}) - 1)\, C_{op}}{(1 - lC_{it} - lC_{mea})^2} < \alpha_\Xi(\boldsymbol{\theta}) \le \dfrac{(2C_{it} + C_{mea})C_{mea}C_{op}}{C_{it}^2}$.

(iv) The V_Ξ*-optimal test plan is*

$$\boldsymbol{\xi}_{V_\Xi} = \left(l, \frac{1 - lC_{mea} - lC_{it}}{C_{op}}, 1 \right)$$

if and only if (a) $2C_{it} + C_{mea} < \dfrac{1}{l} \le 2(C_{it} + C_{mea})$ *and* $0 < \alpha_\Xi(\boldsymbol{\theta}) \le \dfrac{(2l(C_{it} + C_{mea}) - 1)C_{op}}{(1 - lC_{it} - lC_{mea})^2}$

or

(b) $C_{it} + C_{mea} < \dfrac{1}{l} \le 2C_{it} + C_{mea}$ *and* $0 < \alpha_\Xi(\boldsymbol{\theta}) \le \dfrac{lC_{mea}C_{op}}{(1 - lC_{it} - lC_{mea})^2}$.

Corollary 2.3. *When $\alpha(\boldsymbol{\theta}) \to 0$, the V_{Ξ}-optimal test plan is*

$$\boldsymbol{\xi}_{V_{\Xi}} = \left(\frac{1}{2(C_{it} + C_{mea})}, \frac{1}{2C_{op}}, 1 \right)$$

for $2(C_{it} + C_{mea}) < \frac{1}{l}$; otherwise, the V_{Ξ}-optimal test plan is

$$\boldsymbol{\xi}_{V_{\Xi}} = \left(l, \frac{1 - lC_{mea} - lC_{it}}{C_{op}}, 1 \right).$$

Let the parameter function $\alpha_{\Xi}(\boldsymbol{\theta})$ and experimental cost C_{op} be represented by the x-axis and y-axis, respectively. According to the different cost ranges (a) $2(C_{it} + C_{mea}) < \frac{1}{l}$, (b) $2C_{it} + C_{mea} < \frac{1}{l} \leq 2(C_{it} + C_{mea})$, and (c) $C_{it} + C_{mea} < \frac{1}{l} \leq 2C_{it} + C_{mea}$, the feasible regions for the V_{Ξ}-optimal test plans are plotted in Figure 2 using the same colors as in Figure 1. The dividing functions are the necessary and sufficient conditions of the V_{Ξ}-optimal test plan $\boldsymbol{\xi}_{V_{\Xi}}$. Clearly, the slopes of the dividing functions are influenced by the experimental costs C_{it} and C_{mea} in Figure 2. The related properties can be found in Dong and Peng (2025).

The following section introduces the bi-optimal quantile-based test plan that simultaneously satisfies the two criteria.

3 Bi-optimal Quantile-based Test Plan

When the quantity of interest is the q-quantile of a product's lifetime under normal-use conditions S_0 (i.e., $\Xi(\boldsymbol{\theta}) = t_q$), the parameter function in (8) can be seen as a function of q (denoted by $\tilde{\alpha}(q)$) and is referred to as the integrated quantile (IQ) function. The corresponding V_{t_q}-optimal test plan $\boldsymbol{\xi}_{V_{t_q}}$ can be obtained by Theorem 2.2. Hence, a test plan that achieves V_{t_q}-optimality and D-optimality simultaneously is considered. More precisely, if there exists any q such that the optimal decision variables in both (V_{t_q}- and

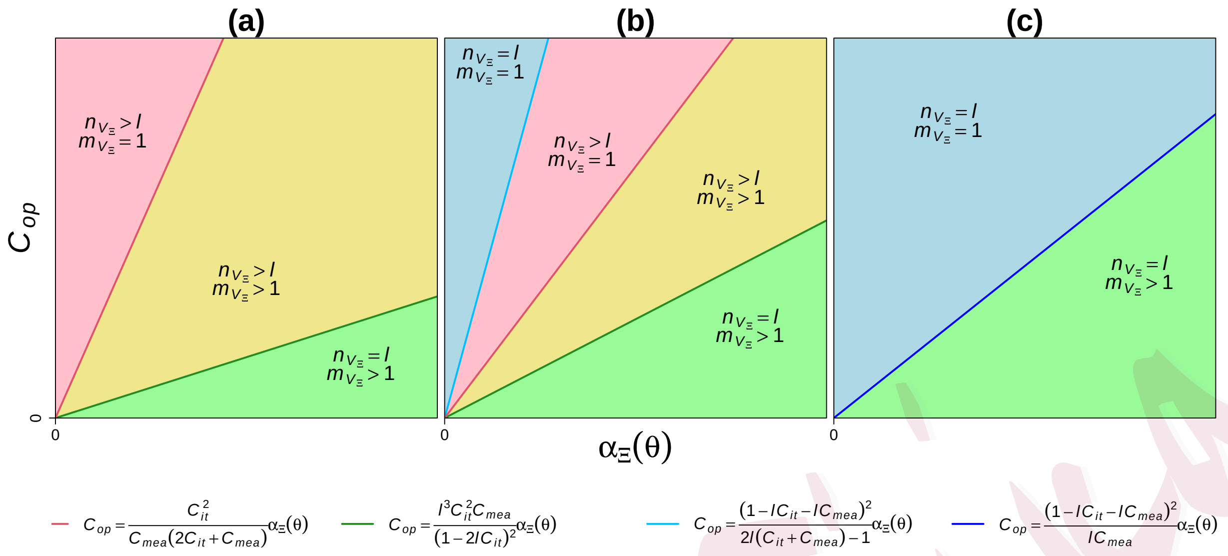

Figure 2: Feasible regions of V_Ξ-optimal test plans (a) $2(C_{it}+C_{mea}) < \frac{1}{l}$, (b) $2C_{it}+C_{mea} < \frac{1}{l} \leq 2(C_{it}+C_{mea})$, and (c) $C_{it}+C_{mea} < \frac{1}{l} \leq 2C_{it}+C_{mea}$

D-) optimality criteria are the same, i.e.,

$$\boldsymbol{\xi}_{V_{t_q}} = \boldsymbol{\xi}_D \;\Leftrightarrow\; n_{V_{t_q}} = n_D,\; t_{m;V_{t_q}} = t_{m,D},\; m_{V_{t_q}} = m_D, \tag{10}$$

then this q is termed as the bi-optimal q^*. The bi-optimal quantile-based test plan is referred to as the $D(q^*)$-optimal test plan (denoted by $\boldsymbol{\xi}_{D(q^*)}$), i.e., $\boldsymbol{\xi}_{D(q^*)} = \boldsymbol{\xi}_{V_{t_{q^*}}} = \boldsymbol{\xi}_D$. Applying Theorems 2.1 and 2.2 to (10) yields a system of three nonlinear equations in the single unknown q. In general, such a system is difficult to solve without imposing additional conditions. However, a solution can be found if the three equations can first be reduced to a single equation. Otherwise, the $D(q^*)$-optimal test plan does not exist. Particularly in the interior case ($n_{D(q^*)} > l$ and $m_{D(q^*)} > 1$), three equations need to be solved under the total cost constraint in (4), which implies that at least an additional condition is required to solve the system of nonlinear equations. In the boundary case (either $n_{D(q^*)} = l$ or $m_{D(q^*)} = 1$), only two equations need to be solved under the total cost constraint (4), so no further conditions are required. In this situation, the bi-optimal q^* can be found from a single equation at the intersection of the feasible regions for the V_{t_q}- and D-optimal test plans. For the trivial case (i.e., $n_{D(q^*)} = l$ and $m_{D(q^*)} = 1$), we have $t_{m;D(q^*)} = (1 - lC_{mea} - lC_{it})/C_{op}$ and no equation needs to be solved for the $D(q^*)$-optimal test plan $\boldsymbol{\xi}_{D(q^*)}$. For the bi-optimal q^*, all that is required is to find the intersection of the feasible regions for both the V_{t_q} and D-optimal test plans.

Here, $D(q^*)$-optimality is considered achieved by simultaneously minimizing the generalized variance of model parameters and approximate variance of the estimated q-quantile of the product's lifetime distribution. If the V_{t_q}-optimal test plan simultaneously satisfies the D-optimality criterion, then the unknown q must satisfy three equations corresponding to three decision variables (i.e., $\boldsymbol{\xi}_{V_{t_q}} = \boldsymbol{\xi}_D$). Hence, it is possible to find the $D(q^*)$-optimal test plan within the same case, as outlined in Theorems 2.1 and 2.2. Otherwise, the $D(q^*)$-optimal test plan does not exist. The feasible region for the existence of a $D(q^*)$-optimal test plan can thus be derived as follows.

Theorem 3.1. *Given $\tilde{\alpha}(q)$, N_0, N_1, N_2, C_{op}, C_{mea}, and C_{it}, the $D(q^*)$-optimal test plan $\boldsymbol{\xi}_{D(q^*)}(= \boldsymbol{\xi}_{V_{t_{q^*}}} = \boldsymbol{\xi}_D)$ can be divided into four cases as follows:*

(i) For $n_{D(q^*)} = l$, $\boldsymbol{\xi}_{D(q^*)}$ exists if and only if $C_{it} + \dfrac{(N_1 + N_2)C_{mea}}{N_2} < \dfrac{1}{l}$, the bi-optimal q^* satisfies

$$\tilde{\alpha}(q^*) = \frac{N_2^2 C_{op}}{N_1^2 l C_{mea}}, \tag{11}$$

and one of the following two conditions: (a) $N_0 \geq N_1 + N_2$, $\dfrac{1}{l} \leq \dfrac{(N_0 + N_1)C_{it}}{N_0 - N_2}$. (b) $N_0 < N_1 + N_2$, $\dfrac{1}{l} \leq \left(2 + \dfrac{N_2}{N_1}\right) C_{it}$.

(ii) For $n_{D(q^*)} > l$ and $m_{D(q^*)} > 1$, $\boldsymbol{\xi}_{D(q^*)}$ exists if and only if $N_0 = N_1 + N_2$, $\dfrac{C_{mea}}{C_{it}} < \dfrac{N_2}{N_1}$,

$C_{it} < \dfrac{N_1}{l(2N_1+N_2)}$ *and the bi-optimal* q^* *satisfies*

$$\tilde{\alpha}(q^*) = \frac{(2N_1+N_2)N_2^2 C_{it} C_{op}}{N_1^3 C_{mea}}. \tag{12}$$

(iii) For $m_{D(q^*)} = 1$, $\boldsymbol{\xi}_{D(q^*)}$ *exists if and only if* $C_{it} + C_{mea} < \dfrac{N_0}{l(N_0+N_1)}$, *the bi-optimal* q^* *satisfies*

$$\tilde{\alpha}(q^*) = \frac{(N_0^2 - N_1^2)C_{op}}{N_1^2}, \tag{13}$$

and one of the following two conditions: (a) $N_0 > N_1 + N_2$ *and* $\dfrac{C_{mea}}{C_{it}} \geq \dfrac{N_0 - N_1}{N_1}$. *(b)* $\max\{N_1, N_2\} < N_0 \leq N_1 + N_2$, $\dfrac{C_{mea}}{C_{it}} \geq \dfrac{N_2}{N_0 - N_2}$.

(iv) For $n_{D(q^*)} = l, m_{D(q^*)} = 1$, $\boldsymbol{\xi}_{D(q^*)}$ *exists if and only if*

(a) $2C_{it} + C_{mea} < \dfrac{1}{l}$, *the bi-optimal* q^* *satisfying*

$$\tilde{\alpha}(q^*) \in \left(0, \frac{(2l(C_{it}+C_{mea})-1)C_{op}}{(1-lC_{it}-lC_{mea})^2}\right], \tag{14}$$

and one of the following conditions:

(1) $\max\{N_1, N_2\} < N_0 < N_1 + N_2$, $C_{it} + C_{mea} \geq \dfrac{N_0}{l(N_0+N_1)}$ *and* $\dfrac{1}{l} \leq C_{it} + \dfrac{(N_1+N_2)C_{mea}}{N_2}$.

(2) $N_0 \leq N_1$, $N_2 < N_1$, $\dfrac{1}{l} \leq C_{it} + \dfrac{(N_1+N_2)C_{mea}}{N_2}$ *and* $\dfrac{1}{l} \leq 2(C_{it} + C_{mea})$.

(3) $N_0 \leq N_2$, $N_1 < N_2$ *and* $\dfrac{1}{l} \leq C_{it} + \dfrac{(N_1+N_2)C_{mea}}{N_2}$,

(4) $N_0 \geq N_1 + N_2$, $C_{it} + C_{mea} \geq \dfrac{N_0}{l(N_0+N_1)}$.

(b) $C_{it} + C_{mea} < \dfrac{1}{l} \leq 2C_{it} + C_{mea}$, $\dfrac{1}{l} \leq C_{it} + \dfrac{(N_1+N_2)C_{mea}}{N_2}$, *the bi-optimal* q^* *satisfying*

$$\tilde{\alpha}(q^*) \in \left(0, \frac{lC_{mea}C_{op}}{(1-lC_{it}-lC_{mea})^2}\right], \tag{15}$$

and one of the following two conditions:

(1) $N_0 > N_1 + N_2$ *and* $C_{it} + C_{mea} \geq \dfrac{N_0}{l(N_0 + N_1)}$.

(2) $N_0 \leq N_1 + N_2$.

Otherwise, the $D(q^*)$*-optimal test plan does not exist.*

We refer to (11)–(13) in Theorem 3.1(i)–(iii) as the DQ-equation. When the DQ-equation holds, the IQ function $\tilde{\alpha}(q^*)$ is only proportional to the experimental costs, which is not related to test configuration. In the following special case $N_0 = N_1 + N_2$, (11)–(13) in Theorem 2.1 can be further simplified into a common DQ-equation.

Corollary 3.1. *For* $N_0 = N_1 + N_2$*, the* DQ*-equation in Theorem 3.1(i)–(iii) is*

$$\tilde{\alpha}(q^*) = \frac{N_2}{N_1} f_D,$$

where the D*-optimal frequency* $f_D = m_D / t_{m;D}$*.*

Corollary 3.1 indicates that the DQ-equation for the $D\left(q^*\right)$-optimal test plan provides the relation of engineering implication (i.e., D-optimal frequency f_D).

According to (14)–(15) in Theorem 3.1(iv), there exists more than one bi-optimal q^*, which is deemed the least interesting case. The bi-optimal q^* with $D(q^*)$-optimality is determined by both the model parameters and experimental costs (see Supplementary Figures 1–3 for feasible regions in Theorem 3.1).

4 IQ Function $\tilde{\alpha}(q)$ Based on the Wiener Process

For the DQ-equation in Theorem 3.1, the IQ function $\tilde{\alpha}(q)$ plays a crucial role in the $D(q^*)$-optimal test plan. There exists more than one solution regarding the unknown q in the DQ-equation. Hence, the IQ function $\tilde{\alpha}(q)$ based on the Wiener process can be investigated to solve the DQ-equation.

In the Wiener process, the lifetime T of a product under normal-use conditions S_0 is defined as the first hitting time when the degradation path $Y(t;S_0)$ crosses the prefixed threshold ω, i.e., $T=\inf\{t|Y(t;S_0)>\omega\}$. The lifetime T follows an IG distribution with mean ω/η and shape parameter ω^2/σ^2, where $\eta=g_1(\beta_0)>0$ and $\sigma^2=g_2(\gamma_0)>0$. The cumulative distribution function (CDF) of T is given by

$$F_T(t;\boldsymbol{\theta})=\Phi\left(\frac{\eta t-\omega}{\sqrt{\sigma^2 t}}\right)+\exp\left(\frac{2\eta\omega}{\sigma^2}\right)\Phi\left(-\frac{\eta t+\omega}{\sqrt{\sigma^2 t}}\right),$$

where Φ is the CDF of the standard normal distribution. When $\Xi(\boldsymbol{\theta})=F_T^{-1}(q;\boldsymbol{\theta})=t_q$, the q-quantile of the product's lifetime can be numerically evaluated by solving $F_T(t_q;\boldsymbol{\theta})=q$. However, since the CDF $F_T(t;\boldsymbol{\theta})$ is analytically intractable, there is no closed-form expression for t_q. Consequently, deriving the explicit expression of $\tilde{\alpha}(q)$ for the $D(q^*)$-optimal test plan is not feasible. Hence, a normalizing logarithmic transformation proposed by Whitmore and Yalovsky (1978) is used to study the bi-optimal quantile-based test plan:

$$Z=\frac{1}{2\rho}+\rho\ln\left(\frac{\eta T}{\omega}\right), \tag{16}$$

where $\rho=\sqrt{\eta\omega/\sigma^2}$ is the signal-to-noise (SN) ratio for the IG distribution. Whitmore and Yalovsky (1978) showed that Z converges in distribution to the standard normal distribution as $\rho\to\infty$. The convergence rate of Z is of the order $1/\rho^2$, which is the square of the coefficient of variation for the IG distribution. When the SN ratio ρ is large, the q-quantile of the lifetime distribution of T for the Wiener process can be approximated as

$$t_q\approx\frac{\omega}{\eta}\exp\left(\frac{\Phi^{-1}(q)}{\rho}-\frac{1}{2\rho^2}\right). \tag{17}$$

The IQ function $\tilde{\alpha}(q)$ in (8), using (17), can then be derived as

$$\tilde{\alpha}(q)=\frac{2\eta^2}{\sigma^2}\left(\frac{1-\rho\Phi^{-1}(q)}{2\rho^2-1+\rho\Phi^{-1}(q)}\right)^2,\ q\in(0,1), \tag{18}$$

which is a continuously differentiable function of q. The properties of $\tilde{\alpha}(q)$ in (18) are depicted in Figure 3.

Proposition 1. *As $0 < \rho < \infty$, the IQ function $\tilde{\alpha}(q)$ is increasing on $(0, \Phi(\rho^{-1} - 2\rho))$ and $(\Phi(\rho^{-1}), 1)$, and decreasing on $(\Phi(\rho^{-1} - 2\rho), \Phi(\rho^{-1}))$. There is an absolute minimum at $q = \Phi(\rho^{-1})$ with $\tilde{\alpha}(\Phi(\rho^{-1})) = 0$. The IQ function $\tilde{\alpha}(q)$ is concave down on $(0, \Phi(z_0))$ and concave up on $(\Phi(z_0), 1)$ with the inflection point at $q = \Phi(z_0)$, where $z_0 = \left(-2\rho(\rho^2 - 1) + \sqrt[3]{(z_1 + \sqrt{27\rho^4\Delta})/2} + \sqrt[3]{(z_1 - \sqrt{27\rho^4\Delta})/2}\right)/(3\rho^2)$ with $z_1 = -2\rho^3(8\rho^6 + 39\rho^4 + 6\rho^2 + 1)$ and the discriminant $\Delta = 4\rho^6(16\rho^6 + 51\rho^4 + 12\rho^2 + 2)$. Moreover, there is a vertical asymptote at $q = \Phi(\rho^{-1} - 2\rho)$ and $\lim_{q\to 0} \tilde{\alpha}(q) = \lim_{q\to 1} \tilde{\alpha}(q) = 2\eta^2/\sigma^2$.*

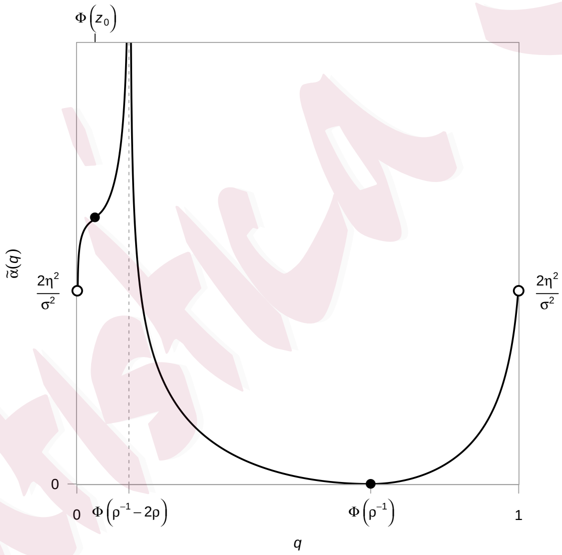

Figure 3: $\tilde{\alpha}(q)$ vs. q

A smaller value for q is of greater interest for product reliability because it provides information on early failures, which in turn offers manufacturers and engineers insights for developing robust maintenance and service strategies. Since the normalizing logarithmic transformation in (16) provides an excellent approximation when the SN ratio ρ is larger than 3 (Whitmore and Yalovsky, 1978), the value of $\Phi(\rho^{-1}-2\rho)$ is less than 10^{-8}. Therefore, to cover the whole range of $\tilde{\alpha}(q)$, the interested interval

$$\left(\Phi\left(\rho^{-1}-2\rho\right), \Phi\left(\rho^{-1}\right)\right), \ \rho < \infty \tag{19}$$

is primarily used to determine the bi-optimal q^* for the Wiener process in practical applications. The inverse function of $\tilde{\alpha}(q)$ is well-defined on the interval $(0, \infty)$. As shown in Supplementary Section 1.7, the bi-optimal q^* using (18) is expressed as

$$q^* = \tilde{\alpha}^{-1}(c) = \Phi\left(\rho^{-1} - \frac{2}{\rho^{-1} + \sqrt{2\eta/(\omega c)}}\right) \quad \text{for } c > 0. \tag{20}$$

Then, a $D(q^*)$-optimal test plan always exists within the interested interval for any C_{it}, C_{mea} and C_{op} as follows:

Theorem 4.1. *Given N_1, N_2, C_{op}, C_{mea}, C_{it}, and (18) for the Wiener process and the interested interval (19) with (20), the $D(q^*)$-optimal test plan can be divided into four cases as follows:*

(i) For $n_{D(q^*)} = l$, $\boldsymbol{\xi}_{D(q^*)}$ uniquely exists if and only if $C_{it} + (N_1+N_2)C_{mea}/N_2 < 1/l$ and $C_{it} \geq N_1/(l(2N_1+N_2))$.

(ii) For $n_{D(q^*)} > l$ and $m_{D(q^*)} > 1$, $\boldsymbol{\xi}_{D(q^*)}$ uniquely exists if and only if $C_{mea}/C_{it} < N_2/N_1$ and $C_{it} < N_1/(l(2N_1+N_2))$.

(iii) For $m_{D(q^*)} = 1$, $\boldsymbol{\xi}_{D(q^*)}$ uniquely exists if and only if $C_{it} + C_{mea} < (N_1+N_2)/(l(2N_1+N_2))$ and $C_{mea}/C_{it} \geq N_2/N_1$.

(iv) For $n_{D(q^*)} = l, m_{D(q^*)} = 1$, $\boldsymbol{\xi}_{D(q^*)}$ exists if and only if

(a) $2C_{it} + C_{mea} < 1/l$ and $C_{it} + C_{mea} \geq (N_1+N_2)/(l(2N_1+N_2))$ or

(b) $2C_{it} + C_{mea} \geq 1/l$, $C_{it} + C_{mea} < 1/l$ *and* $C_{it} + (N_1 + N_2)C_{mea}/N_2 \geq 1/l$.

Furthermore, the bi-optimal q^* *for (i)–(iii) is* $q^* = \tilde{\alpha}^{-1}(N_2 f_D/N_1)$. *For the (iv), there are infinite bi-optimal* q^**s:*

(a) $q^* \in \left[\tilde{\alpha}^{-1}\left(\frac{(2l(C_{it}+C_{mea})-1)C_{op}}{(1-lC_{it}-lC_{mea})^2}\right), \Phi(\rho^{-1})\right)$ *or*

(b) $q^* \in \left[\tilde{\alpha}^{-1}\left(\frac{lC_{mea}C_{op}}{(1-lC_{it}-lC_{mea})^2}\right), \Phi(\rho^{-1})\right)$.

Since the function $\tilde{\alpha}^{-1}$ is decreasing, Theorem 4.1(i)–(iii) indicates that a higher D-optimal frequency results in a smaller the bi-optimal q^*.

Based on the proposed bi-optimal quantile-based test plan, the test configuration for ADTs can be determined numerically in the following section.

5 Test Configuration in ADTs

Tseng and Lee (2016) indicated that, for a three-level allocation problem using the Wiener process, the V_{t_q}-optimal sample size allocation exists only for $l = 2$, with the highest stress level always included. Therefore, following the assumptions on the test configuration for ADTs proposed by Lee et al. (2020), the V_{t_q}-optimal test configuration determines the sample size allocation, stress levels, and termination time at each stress level for $l = 2$. For the Wiener process, the simple exp-linear relationship between the mean drift rate and a specific accelerating variable, and the constant function for the diffusion coefficient are assumed, i.e., $g_1(\boldsymbol{X}_k'\boldsymbol{\beta}) = \exp(\beta_0 + \beta_1 X_{k,1})$ and $g_2(\boldsymbol{Z}_k'\boldsymbol{\gamma}) = \gamma_0$, respectively. Hence, we have $(N_0, N_1, N_2) = (3, 2, 1)$ and $\boldsymbol{\theta} = (\beta_0, \beta_1, \gamma_0)'$. As long as the experimental costs (C_{mea}, C_{op}, C_{it}) and parameter estimates are given, the $D(q^*)$-optimal test plan $\boldsymbol{\xi}_{D(q^*)} = (n_{D(q^*)}, t_{m;D(q^*)}, m_{D(q^*)})$ and bi-optimal q^* can be obtained directly from Theorem

4.1. Furthermore, the $D(q^*)$-optimal test plan depends only on the experimental costs and is not related to the test configuration.

For $l = 2$, the sample proportions are $(p_1, 1-p_1)$. The two standardized accelerating variables are $(X_{1,1}, X_{2,1}) = (x_{1,1}, 1)$ within the range of stress level $(x_L, 1)$, where x_L is a given fixed lower bound. The termination time at S_k is defined as $t_{m,k} = t_U r_k m$, where t_U is a unit of time and r_k is the number of units of time at S_k. The corresponding ratio of two termination times is $u = r_1/r_2$, which is not related to t_U and m. Let $\Xi(\boldsymbol{\theta}) = t_{q^*}$, then the approximate variance of $\hat{t}_{q^*}$ is given by

$$\begin{aligned}\mathrm{AVar}(\hat{t}_{q^*}) &= \frac{1}{n_{D(q^*)}}\left(\frac{2\gamma_0^2\,(\partial t_{q^*}/\partial\gamma_0)^2}{m_{D(q^*)}} + \frac{\gamma_0\exp(-2\beta_0)\,(\partial t_{q^*}/\partial\beta_0)^2}{t_{m;D(q^*)}}H(p_1, x_{1,1}, u)\right)\\ &\propto \frac{1}{n_{D(q^*)}}\left(\frac{1}{t_{m;D(q^*)}} + \frac{\alpha_{t_{q^*}}(\boldsymbol{\theta})}{m_{D(q^*)}}\right),\end{aligned}$$

where

$$\begin{aligned}H(p_1, x_{1,1}, u) &= \frac{(1+u)\left\{up_1x_{1,1}^2\exp(2\beta_1x_{1,1}) + (1-p_1)\exp(2\beta_1)\right\}}{up_1(1-p_1)(1-x_{1,1})^2\exp\left(2\beta_1(1+x_{1,1})\right)} \quad \text{and} \\ \alpha_{t_{q^*}}(\boldsymbol{\theta}) &= \frac{2\gamma_0\exp(2\beta_0)\,(\partial t_{q^*}/\partial\gamma_0)^2}{H(p_1, x_{1,1}, u)\,(\partial t_{q^*}/\partial\beta_0)^2}.\end{aligned} \tag{21}$$

Consequently, the $D(q^*)$-optimal test plan can be obtained directly, which eliminates the computation time needed for a grid-search procedure in Section 4 proposed by Lee et al. (2020). Given the parameter estimates and $D(q^*)$-optimal test plan, finding the $V_{t_{q^*}}$-optimal test configuration $(p_1^*, x_{1,1}^*, u^*)$ by minimizing $\mathrm{AVar}(\hat{t}_{q^*})$ is equivalent to minimizing $H(p_1, x_{1,1}, u)$ subject to

$$\frac{1}{n_{D(q^*)}} \le p_1 \le \frac{n_{D(q^*)}-1}{n_{D(q^*)}},\ x_L \le x_{1,1} \le 1,\ \text{and}\ \frac{f_{D(q^*)}t_U}{1-f_{D(q^*)}t_U} \le u \le \frac{1-f_{D(q^*)}t_U}{f_{D(q^*)}t_U}, \tag{22}$$

where $f_{D(q^*)} = m_{D(q^*)}/t_{m;D(q^*)}$. Due to the complicated structure of $H(p_1, x_{1,1}, u)$, it is challenging to obtain an explicit expression for each test configuration. However, the $V_{t_{q^*}}$-optimal test configuration $(p_1^*, x_{1,1}^*, u^*)$ for $l = 2$ benefits from relying on numerical search methods. Based on the definition of ψ_k in Section 2, the relation between ψ_1 and u is $u = \psi_1/(1-\psi_1)$. Therefore, the $V_{t_{q*}}$-optimal ψ_1^* can be obtained from $\psi_1^* = u^*/(1+u^*)$.

6 Applications

The following examples are presented to demonstrate the practical applicability of the previous theoretical analysis.

Example 6.1. Gallium arsenide (GaAs) laser data (Meeker et al., 2022, example 20.1) are used to demonstrate the $D(q^*)$-optimal test plan under a total cost constraint using the Wiener process (i.e., $(N_0, N_1, N_2) = (2, 1, 1)$). According to Cheng and Peng (2012), the ML estimates of the unknown parameters are $(\hat{\eta}, \hat{\sigma}) = (2.04 \times 10^{-3}, 1.27 \times 10^{-2})$ and the threshold is $\omega = 10$. The SN ratio is estimated to be 11.28, which is sufficiently large for this case. For illustrative purposes, the link functions g_1 and g_2 are chosen as constant functions,

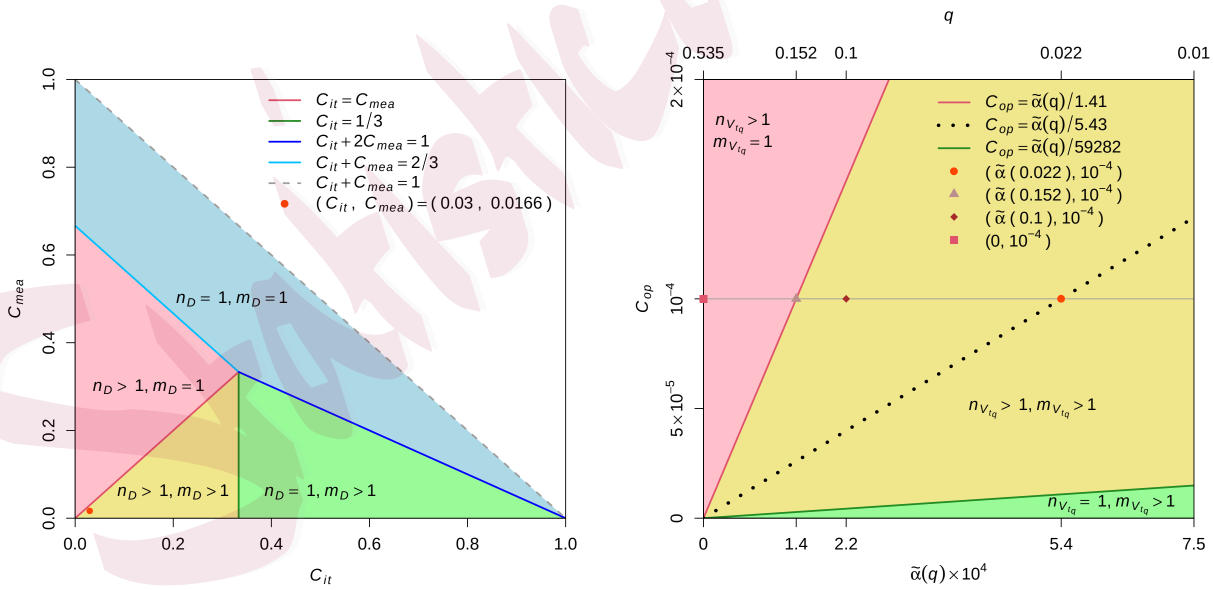

(a) C_{mea} vs. C_{it} (b) C_{op} vs. $\tilde{\alpha}(q)$

Figure 4: $D(q^*)$-optimal test plan for the GaAs laser data

and the experimental costs are set to $(C_{it}, C_{mea}, C_{op}) = (0.03, 0.0166, 10^{-4})$. Based on the experimental costs $(C_{it}, C_{mea}) = (0.03, 0.0166)$, Figure 4(a) shows that the D-optimal test plan is the interior case and $\boldsymbol{\xi}_D = (11.11, 3333.33, 1.81)$ by Theorem 2.1(i)-(2). Since $2(C_{it} + C_{mea}) = 0.093 < 1$, Figure 4(b) illustrates the necessary and sufficient conditions for the V_{t_q}-optimal test plan by Theorem 2.2, where the second x-axis represents the value of q. When $C_{op} = 10^{-4}$, the V_{t_q}-optimal test plan is the interior case by Theorem 2.2(ii) for $q \in [0.01, 0.152]$ and boundary case by Theorem 2.2(iii) for $q \in (0.152, 0.535]$. Since the D-optimal test plan is the interior case by Theorem 3.1(ii), the black dotted line indicating $C_{op} = \tilde{\alpha}(q)C_{mea}/(3C_{it}) = \tilde{\alpha}(q)/5.43$ represents the DQ equation in (12). The point of intersection between $C_{op} = 10^{-4}$ and $C_{op} = \tilde{\alpha}(q)/5.43$ manifests at $(5.4 \times 10^{-4}, 10^{-4})$. By Theorem 4.1(ii), the bi-optimal q^* is $\tilde{\alpha}^{-1}(5.4 \times 10^{-4}) = 0.022$ and the $D(q^*)$-optimal test plan is $\boldsymbol{\xi}_{D(0.022)} = (11.11, 3333.33, 1.81)$.

In practice, the optimal integers n and m can be obtained using Theorems 2.1 and 2.2 as the starting point for discrete search algorithms (e.g., Taha, 2017). Using the grid-search method, the D- and $V_{t_{0.022}}$-optimal test plans are found as $\boldsymbol{\xi}_D^\diamond = (11, 3056.54, 2)$ and $\boldsymbol{\xi}_{V_{t_{0.022}}}^\diamond = (10, 3687.76, 2)$, respectively, which are quite close to the $D(q^*)$-optimal test plan $\boldsymbol{\xi}_{D(0.022)}$. The D- and V_{t_q}-efficiencies at the experimental costs $(C_{op}, C_{mea}, C_{it})$ can be defined as

$$\mathrm{Eff}_D(\boldsymbol{\xi}) = \left\{ \frac{\mathbb{D}(\boldsymbol{\xi})}{\mathbb{D}(\boldsymbol{\xi}_D)} \right\}^{\frac{1}{N_1+N_2}} \quad \text{and} \quad \mathrm{Eff}_{V_{t_q}}(\boldsymbol{\xi}) = \frac{\mathbb{V}_{t_q}(\boldsymbol{\xi}_{V_{t_q}})}{\mathbb{V}_{t_q}(\boldsymbol{\xi})}, \tag{23}$$

respectively. The corresponding D- and $V_{t_{0.022}}$-efficiencies under the experimental costs $(C_{it}, C_{mea}, C_{op}) = (0.03, 0.0166, 10^{-4})$ are $\mathrm{Eff}_D(\boldsymbol{\xi}_D^\diamond) = 99.6\%$ and $\mathrm{Eff}_{V_{t_{0.022}}}(\boldsymbol{\xi}_{V_{t_{0.022}}}^\diamond) = 99.5\%$, respectively.

For a typical fixed value of q (e.g., $q = 0.1$), the IQ function and $V_{t_{0.1}}$-optimal test plan are $\tilde{\alpha}(0.1) = 2.17 \times 10^{-4}$ from (18) and $\boldsymbol{\xi}_{V_{t_{0.1}}} = (12.49, 3745.95, 1.21)$ by Theorem 2.2(ii), respectively. Based on the V_{t_q}-efficiency defined in (23), the corresponding $V_{t_{0.1}}$-efficiency of the $D(q^*)$-optimal test plan (i.e., $\boldsymbol{\xi}_{V_{t_{0.1}}}$ versus $\boldsymbol{\xi}_{D(0.022)}$) is

$$\text{Eff}_{V_{t_{0.1}}}(\boldsymbol{\xi}_{D(0.022)}) = \frac{\mathbb{V}_{t_{0.1}}(\boldsymbol{\xi}_{V_{t_{0.1}}})}{\mathbb{V}_{t_{0.1}}(\boldsymbol{\xi}_{D(0.022)})} = \frac{\frac{1}{12.49}\left(\frac{1}{3745.95} + \frac{2.17\times 10^{-4}}{1.21}\right)}{\frac{1}{11.11}\left(\frac{1}{3333.33} + \frac{2.17\times 10^{-4}}{1.81}\right)} = 94.50\%.$$

The result shows that the $D(q^*)$-optimal test plan is also highly efficient for a typical fixed value $q = 0.1$. Note that the bi-optimal q^* is determined by the given experimental costs and the pre-specified values of the model parameters (refer to (20)). Therefore, it may not be close to a typical fixed value of q. For example, if the experimental costs are changed to $(C_{mea}, C_{op}, C_{it}) = \left(1.45 \times 10^{-3}, 10^{-4}, 3.6 \times 10^{-3}\right)$, the $V_{t_{0.1}}$-optimal test plan is $\xi_{V_{t_{0.1}}} = (107.6,\ 3873.75,\ 1.44)$. Using (20), the bi-optimal $q^* = 0.01$, which is not very close to the typical fixed value $q = 0.1$. Nevertheless, the corresponding $V_{t_{0.1}}$-efficiency of the $D(q^*)$-optimal test plan (i.e., $\xi_{D(0.01)} = (92.59,\ 3333.33,\ 2.48)$) is still 90.7%.

Under the experimental costs $(C_{it}, C_{mea}, C_{op}) = (0.03, 0.0166, 10^{-4})$, a practical range for q can be naively chosen as [0.01,0.152] (i.e., the interior case). Figure 5 shows the D-efficiency defined in (23) of the V_{t_q}-optimal test plan for this range. For each q, the V_{t_q}-optimal test plan, $\boldsymbol{\xi}_{V_{t_q}}$, can be obtained by Theorem 2.2. For the typical fixed value $q = 0.1$, the D-efficiency of $\boldsymbol{\xi}_{V_{t_{0.1}}}$ is evaluated as

$$\text{Eff}_D(\boldsymbol{\xi}_{V_{t_{0.1}}}) = \left\{\frac{\mathbb{D}(\boldsymbol{\xi}_{V_{t_{0.1}}})}{\mathbb{D}(\boldsymbol{\xi}_D)}\right\}^{\frac{1}{N_1+N_2}} = \sqrt{\frac{12.49^2 \times 3745.95 \times 1.21}{11.11^2 \times 3333.33 \times 1.81}} = 97.48\%.$$

In addition, Figure 5 demonstrates that the D-efficiency for $\boldsymbol{\xi}_{V_{t_q}}$ is above 90% for all q in this range. How to reconcile the discrepancy between the computed q^* and the value of q suggested by the business owner deserves further study.

Example 6.2. We use the stress relaxation data with a single accelerating variable (i.e., temperature) from Yang (2007) to illustrate the $D(q^*)$-optimal test plan and $V_{t_{q^*}}$-optimal

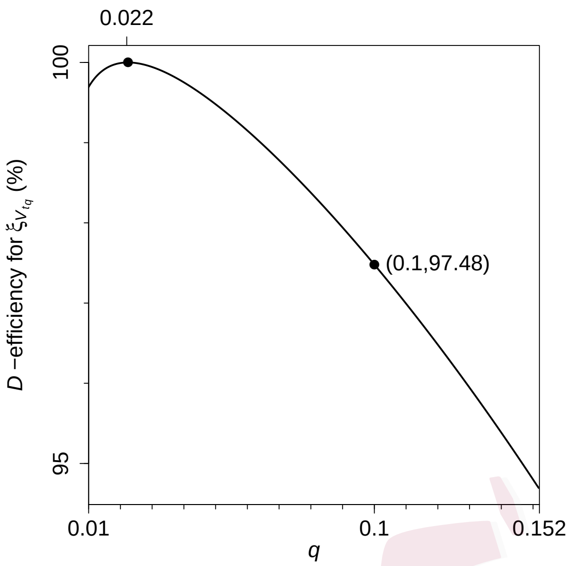

Figure 5: D-efficiencies of $\boldsymbol{\xi}_{V_{t_q}}$ over $q \in [0.01, 0.152]$ for the GaAs laser data under $(C_{it}, C_{mea}, C_{op}) = (0.03, 0.0166, 10^{-4})$

test configuration obtained by the Wiener process (i.e., $(N_0, N_1, N_2) = (3, 2, 1)$) under the total cost constraint in (4). According to Table 3 in Tseng and Lee (2016), the ML estimates of the unknown parameters under a normal use condition (i.e., $S_0 = 40°\text{C}$) are $(\hat{\eta}, \hat{\sigma}) = (\exp(\hat{\beta}_0), \sqrt{\hat{\gamma}_0}) = (\exp(-2.0709), \sqrt{1/3.7481}) = (0.126, 0.517)$ and $\hat{\beta}_1 = 1.9745$ with the threshold $\omega = 30$. The SN ratio is estimated to be 3.77, which is sufficiently large for this case. Given the experimental costs $(C_{it}, C_{mea}, C_{op}) = (0.05, 5 \times 10^{-4}, 1.008 \times 10^{-4})$ and $l = 2$, the conditions $C_{mea} = 5 \times 10^{-4} < N_2 C_{it}/(N_0 - N_2) = 0.025$ and $C_{it} = 0.05 < (N_0 - N_2)/(l(N_0 + N_1)) = 0.2$ in Theorem 4.1(ii) are satisfied (i.e., the interior case). Therefore, by Corollary 3.1 and Theorem 4.1(ii), the bi-optimal $q^* = \tilde{\alpha}^{-1}(f_D/2) = 0.02$, where the D-optimal frequency is $f_D = N_2(N_0 + N_1)C_{it}C_{op}/(N_1(N_0 - N_2)C_{mea}) = 0.0126$. The $D(q^*)$-optimal test plan, $\boldsymbol{\xi}_{D(0.02)} = (8, 3968.25, 50)$, achieves 100% efficiency for two optimality criteria. The $D(q^*)$-optimal test plan can be used to gather more information about model parameters and more precisely estimate the q^*-quantile of the product lifetime distribution at $S_0 = 40°\text{C}$.

Following assumptions of the test configuration at $l = 2$ and $t_U = 1$ in Lee et al. (2020), the temperature range is set to (50°C, 100°C). Based on the Arrhenius law, the lower bound of the testing standardized stress level is

$$x_L = \frac{1/(273.15 + 40) - 1/(273.15 + 50)}{1/(273.15 + 40) - 1/(273.15 + 100)} = 0.1925.$$

The $V_{t_{q^*}}$-optimal test configuration $(p_1^*, x_{1,1}^*, u^*)$ can then be obtained numerically by minimizing $H(p_1, x_{1,1}, u)$ in (21) subject to the following constraints

$$\frac{1}{8} \leq p_1 \leq \frac{7}{8}, \quad 0.1925 \leq x_{1,1} \leq 1, \text{ and } \frac{0.0126}{1 - 0.0126} \leq u \leq \frac{1 - 0.0126}{0.0126}.$$

Therefore, the $V_{t_{q^*}}$-optimal test configuration is $(p_1^*, x_{1,1}^*, u^*) = (0.875, 0.2113, 8.4909)$ with $H(p_1^*, x_{1,1}^*, u^*) = 0.997$ by using the function `optim` in R (R Core Team 2025). Table 2 presents the unit-scale and original-scale values for the $V_{t_{q^*}}$-optimal test configuration based on the $D(q^*)$-optimal test plan $\boldsymbol{\xi}_{D(0.02)} = (8, 3968.25, 50)$, where $\psi_1^* = u^*/(1 + u^*) = 0.895$. A larger sample size allocation p_1^* (i.e., upper bound) and a longer termination time $t_{m,1}^*$ increase the importance of the optimal stress level $x_{1,1}^*$, which is close to x_L.

7 Concluding Remarks

Under a total cost constraint, we propose a bi-optimal quantile-based test plan for the Wiener process. The value of q is chosen based on a secondary optimality criterion (i.e., it is problem-driven), with the aim of improving product reliability (i.e., engineering implication) while ensuring effective resource allocation (i.e., business considerations). The proposed innovation is practically applicable and provides manufacturers with insights for developing robust maintenance and service strategies. The given fixed q and bi-optimal q^*

$D(q^*)$-Optimal Test Plan	$V_{t_{q^*}}$-Optimal Test Configuration	
$\boldsymbol{\xi}_{D(q^*)}$	Unit Scale	Original Scale
$q^* = 0.02$	$x^*_{1,1} = 0.2113$	51.01°C
$n_{D(q^*)} = 8$	$p^*_1 = 0.875$	$(n^*_1, n^*_2) = (7, 1)$
$t_{m;D(q^*)} = 3968.25$	$\psi^*_1 = 0.895$	$(t^*_{m,1}, t^*_{m,2}) = (3550.14, 418.11)$
$m_{D(q^*)} = 50$	–	$(m_{D(q^*)}, m_{D(q^*)}) = (50, 50)$

Table 2: $D(q^*)$-optimal test plan and $V_{t_{q^*}}$-optimal test configuration with $l = 2$ for the stress relaxation data.

can be viewed as playing roles analogous to the pre-specified significance level α (often 5%) and the p-value in statistical hypothesis testing. The existence of a $D(q^*)$-optimal test plan is established in Theorem 3.1. Furthermore, by using a normalizing logarithmic transformation for the Wiener process, we show that a $D(q^*)$-optimal test plan always exists and is unique within the interested interval, except in the trivial case. The ADT model based on the Wiener process in (1) offers a clear and intuitive interpretation of the bi-optimal quantile-based test plan. The $V_{t_{q^*}}$-optimal test configuration for the ADT can be found using numerical search methods in practical applications.

It is an important and challenging problem to determine an optimal test plan for a given fixed q that appropriately balances between the two objectives. A promising avenue for future research is the theoretical and numerical investigation of multi-optimal quantile-based test plans.

References

[1] Atkinson, A. C., Donev, A. N., and Tobias, R. D. (2007), *Optimum Experimental Designs, with SAS*, New York: Oxford University Press.

[2] Bagdonavičius, V. and Nikulin, M. S. (2001), *Accelerated Life Models: Modeling and Statistical Analysis*, Boca Raton: Chapman & Hall/CRC.

[3] Boulanger, M. and Escobar, L. A. (1994), Experimental design for a class of accelerated degradation tests. *Technometrics*, **36**, 260–272.

[4] Cheng, Y. S., Chen, Y., and Lee, M. L. T. (2025), Longitudinal survival analysis using first hitting time threshold regression: with applications to Wiener processes. *Stats*, **8**, Article 32.

[5] Cheng, Y. S. and Peng, C. Y. (2012), Integrated degradation models in R using iDEMO. *Journal of Statistical Software*, **49**, 1–22.

[6] Cheng, Y. S. and Peng, C. Y. (2024), Optimal test planning for heterogeneous Wiener processes. *Naval Research Logistics*, **71**, 509–520.

[7] Chernoff, H. (1953), Locally optimal designs for estimating parameters. *Annals of Mathematical Statistics*, **24**, 586–602.

[8] Chhikara, R. S. and Folks, L. (1989), *The Inverse Gaussian Distribution: Theory, Methodology, and Applications*, New York: Marcel Dekker.

[9] D'Hondt, M., Fedorova, M., Peng, C. Y., Gevaert, B., Taevernier, L., Hoffmann, R., and De Spiegeleer, B. (2014), Dry heat forced degradation of buserelin peptide: Kinetics and degradant profiling. *International Journal of Pharmaceutics*, **467**, 48–59.

[10] Dong, Y. S. and Peng, C. Y. (2025), Importance inference of optimal test planning for degradation analysis. *IEEE Transactions on Reliability*, **74**, 4426–4440.

[11] Hu, C. H., Lee, M. Y., and Tang, J. (2015), Optimum step-stress accelerated degradation test for Wiener degradation process under constraints. *European Journal of Operational Research*, **241**, 412–421.

[12] Lee, I. C., Tseng, S. T., and Hong, Y. (2020), Global planning of accelerated degradation tests based on exponential dispersion degradation models. *Naval Research Logistics*, **67**, 469–483.

[13] Liao, C. M. and Tseng, S. T. (2006), Optimal design for step-stress accelerated degradation tests. *IEEE Transactions on Reliability*, **55**, 59–66.

[14] Lim, H. (2015), Optimum accelerated degradation tests for the gamma degradation process case under the constraint of total cost. *Entropy*, **17**, 2556–2572.

[15] Lim, H. and Yum, B. J. (2011), Optimal design of accelerated degradation tests based on Wiener process models. *Journal of Applied Statistics*, **38**, 309–325.

[16] Meeker, W. Q., Escobar, L. A., and Pascual, F. G. (2022), *Statistical Methods for Reliability Data* (2nd ed.), New York: John Wiley & Sons.

[17] Nelson, W. B. (2004), *Accelerated Testing: Statistical Models, Test Plans, and Data Analysis*, New York: John Wiley & Sons.

[18] Peng, C. Y. and Cheng, Y. S. (2021), Profile optimum planning for degradation analysis. *Naval Research Logistics*, **68**, 951–962.

[19] Prasad, M., Gopika, V., and Shridharan, A. (2020), Application of Hougaard stochastic model for flow-accelerated corrosion wall thinning in an orifice. *Life Cycle Reliability and Safety Engineering*, **9**, 349–352.

[20] Prasad, M., Gopika, V., Sridharan, A., Parida, S., and Gaikwad, A. J. (2018), Hougaard process stochastic model to predict wall thickness in flow accelerated corrosion. *Annals of Nuclear Energy*, **117**, 247–258.

[21] Pukelsheim, F. (1993), *Optimal Design of Experiments*, New York: John Wiley & Sons.

[22] R Core Team (2025), R: a language and environment for statistical computing, Vienna: R foundation for statistical computing. Available at http://www.R-project.org/

[23] Taha, H. A. (2017), *Operations Research: An Introduction* (10th ed.), New York: Pearson Education.

[24] Tsai, C. C., Tseng, S. T., and Balakrishnan, N. (2012), Optimal design for gamma degradation processes with random effects. *IEEE Transactions on Reliability*, **61**, 604–613.

[25] Tseng, S. T. and Lee, I. C. (2016), Optimum allocation rule for accelerated degradation tests with a class of exponential-dispersion degradation models. *Technometrics*, **58**, 244–254.

[26] Tseng, S. T., Tsai, C. C., and Balakrishnan, N. (2011), Optimal sample size allocation for accelerated degradation test based on Wiener process, in: Balakrishnan N. (ed.).

Methods and Applications of Statistics in Engineering, Quality Control, and the Physical Sciences. New York: John Wiley & Sons, 330–343.

[27] Wang, Y. H. and Wong, S. H. D. (2015), Modelling accelerated degradation test and shelf-life prediction of dye-sensitized solar cells with different types of solvents. *Solar Energy*, **118**, 600–610.

[28] Whitmore, G. A. and Yalovsky, M. (1978), A normalizing logarithmic transformation for inverse Gaussian random variables. *Technometrics*, **20**, 207–208.

[29] Wu, S. J. and Chang, C. T. (2002), Optimal design of degradation tests in presence of cost constraint. *Reliability Engineering and System Safety*, **76**, 109–115.

[30] Wu, C. F. J. and Hamada, M. (2021), *Experiments: Planning, Analysis, and Optimization* (3rd ed.), New York: John Wiley & Sons.

[31] Yang, C. H., Hsu, Y. H., and Hu, C. H. (2024), Mis-specification analyses and optimum degradation test plan for Wiener and inverse Gaussian processes. *Communications in Statistics—Theory and Methods*, **53**, 700–717.

[32] Yang, G. (2007), *Life Cycle Reliability Engineering*, New York: John Wiley & Sons.

[33] Yu, H. F. and Tseng, S. T. (1999), Designing a degradation experiment. *Naval Research Logistics*, **46**, 689–706.